Estimation of Upwelling SW and LW for Cape Don and Garden Point using Darwin Data

Chuck Long
Atmospheric Radiation Measurement Program
Pacific Northwest National Laboratory
P. O. 999, MSIN: K9-24
Richland, WA, USA 99352
Ofc.: 1 (509) 372-4917
FAX: 1 (509) 372-6247
e-mail: chuck.long@pnl.gov

Introduction

The small radiometer systems deployed at cape Don and Garden Point during TWP-ICE included upward facing shortwave (SW) and longwave (LW) radiometers only to measure the downwelling SW (SWdn) and LW (LWdn). The Variational Analysis methodology, however, requires the upwelling SW (SWup) and LW (LWup) components. As such, I have been asked if there is any way of estimating the upwelling SW and LW for these sites. In an attempt to do this I have developed relationships using data from the ARM Darwin site, and applied those relationships to the Cape Don and Garden Point data. While I can estimate how well these relationships do in reproducing the Darwin data, the additional uncertainty when they are applied to the other two sites depends on to what extent the surface in the field-of-view of the Darwin downward facing radiometers represents the surfaces at Cape Don and Garden Point (or the Darwin area itself, for that matter), which is unknown. Nevertheless, the estimated values are generated in the spirit of “they are in the ball park” and “something in the ball park is better than nothing at all.”

Views of Darwin, Garden Point, and Cape Don

Figure 1 shows a picture of the Darwin site taken by Jim Mather out the window of a commercial aircraft as it was taking off from Darwin airport in November of 2004. Figure 2 is a similar photo taken by myself on February 2, 2006 during TWP-ICE. In both photos a red circle has been drawn around the met tower on which the downward facing SW and LW radiometers are mounted at a height of about 9 meters or so. Figure 3 shows a picture of the met tower and radiometers mounted on a cross piece so that they are about 2-3 meters out from the tower. Figure 4 shows another view of the instrument runway at the Darwin ARM site looking away from the BoM Met Office building, with the met tower cross boom just visible on the upper left of the image. As these photos show, the downward facing SW and LW radiometers at Darwin have bare ground consisting of reddish soil and gravel directly below them, with some vegetation scattered about in the field-of-view, primarily grass. The bare instrument runway is raised to facilitate drainage during the wet season so that the Darwin ARM technicians can do the daily rounds without slogging through swampy ground. As is always the case with upwelling measurements, and as the photos in Figures 1 through 4 show, the question of how representative these Darwin upwelling radiation measurements are of the larger scale area is subject to debate.

Figure 1: Aerial photo of the Darwin ARM site taken in November of 2004.

Figure 2: Aerial photo of the Darwin ARM site taken on February 2, 2006.

Figure 3: Photo of the met tower and cross boom at the Darwin ARM site.

Figure 4: Another view of the instrument runway at the Darwin ARM site.

Figures 5 through 7 show aerial views of the Cape Don site, with Figure 7 showing a closer view. The Cape Don site is on a peninsula surrounded by sea (Figs.5 and 6), thus the question of the larger scale “representative surface” is a bit convoluted. On the small scale, the radiometer system itself (location circled in red in Figure 7) sat on surface very similar to that in the field-of-view of the Darwin upwelling radiometers, consisting of reddish soil and gravel, with scattered grassy vegetation. The larger cleared area of the Cape Don lodge was more covered in grassy vegetation, with most of the surrounding peninsula then primarily forested.

Similarly, Figures 8 through 10 show aerial views of the Garden Point site, with Figure 10 showing a closer view. As Figure 8 shows, Garden Point borders a sea passage separating the two islands. The proximity of the town to the passage is shown in Figure 9. Figure 10 shows a close-up view of the site, with the radiometer system circled in red. Again there is some similarity between the area immediately surrounding the radiometer stand and the Darwin downward facing radiometer view, i.e. reddish dirt/gravel and grassy vegetation.

For all three sites, then, the surface properties in the immediate vicinity of the radiation measurements are similar. Thus the relationships determined using the Darwin data likely have some reasonable applicability at Cape Don and Garden Point for the immediate area. But again in all three cases exactly what these measurements represent in relation to the larger surrounding area is a good question.

Figure 5: Google Earth view showing the Cape Don site location and surrounding sea.

Figure 6: Aerial view from afar of Cape Don site showing surrounding sea.

Figure 7: Closer aerial view of Cape Don site, radiometer system circled in red.

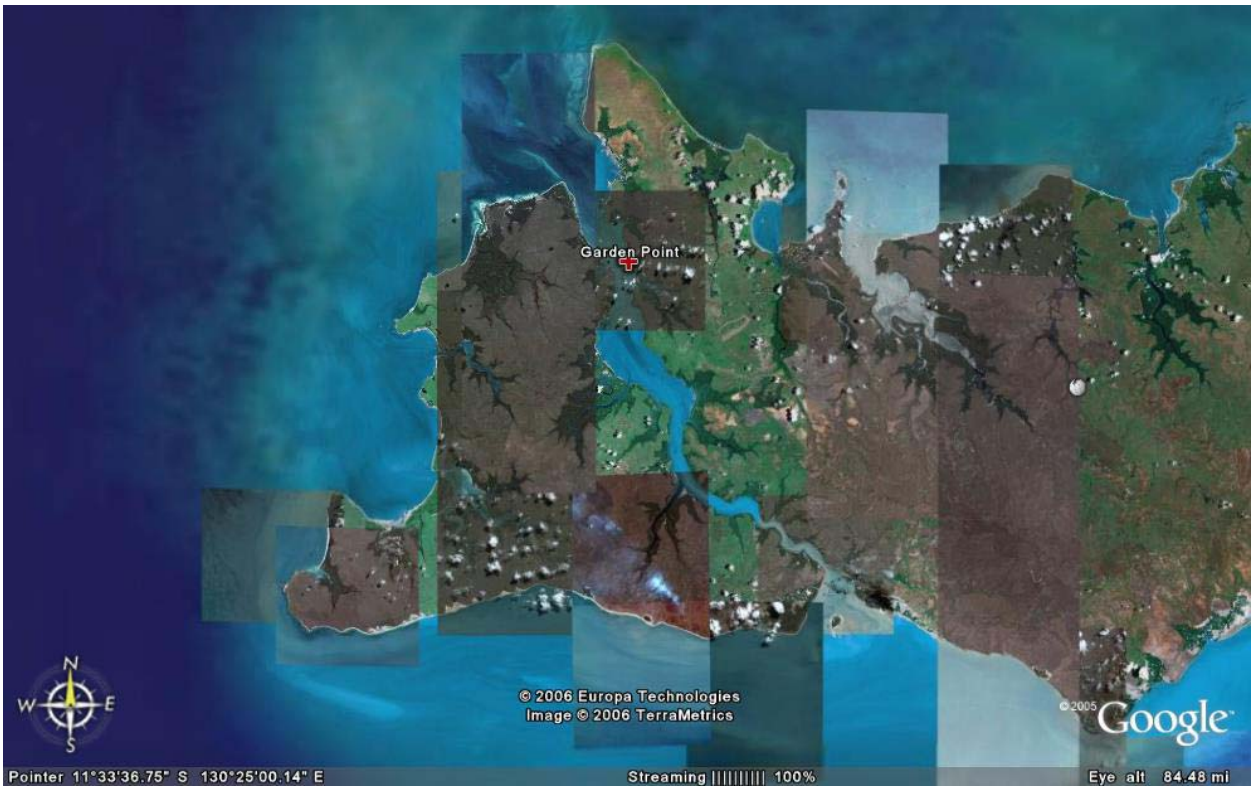

Figure 8: Google Earth view showing the Garden Point site location.


Figure 9: Aerial view from afar of Garden Point site showing nearby sea.


Figure 10: Closer aerial view of Garden Point site, radiometer system circled in red.

Upwelling SW Relationship Determined Using Darwin Data

One typical aspect of surface SW albedo (reflectivity) is that there is often a solar zenith angle dependence for times when the sun is not blocked by cloud, i.e. there is a large amount of incident SW coming from a relatively small portion of the sky (Long, 2005). For times when the direct sun is blocked, the incident radiation field exhibits far less angular variability, thus naturally the surface albedo tends to remain fairly constant with respect to solar zenith angle.

Figure 11 shows a plot of 15-minute averages of the measured surface albedo, calculated as SWup divided by the SWdn, using data including and surrounding the TWP-ICE period spanning from 20051223 through 20060421 in order to provide a statistically robust dataset. The data are separated by the portion of the total downwelling SW that is due to the direct component. The “direct albedo” is defined as that for which the ratio of direct SWdn over total SWdn is greater than or equal to 15%, and the “diffuse albedo” is defined as that wherein the direct over total SWdn ratio is less than 15%. As Figure 11 shows, the diffuse albedo is fairly constant across the range of solar zenith angles, with an average value of about 14% (referenced to the left hand Y axis). The direct albedo exhibits some solar zenith angle dependence, with an RMS fitted line going from a bit less than 15% for overhead sun increasing to about 18% for solar zenith angles of around 80 degrees (CosZ = 0.17). The linear fit is shown in the upper right of the plot.

Thus, in order to estimate SWup from SWdn measurements, first the ratio of direct SWdn over total SWdn (Dir/Tot) is calculated. Then:

For Dir/Tot < 0.15:

$$SWup = 0.14 * SWdn \quad (1)$$

For Dir/Tot ≥ 0.15:

$$SWup = (0.179 - 0.0319 * \mu_0) * SWdn \quad (2)$$

Where μ_0 is the cosine of the solar zenith angle.

Equations (1) and (2) were applied to the Darwin SWdn data, and the comparison of estimated to measured SWup is shown in Figure 12. An RMS fitted line through the comparison forced through zero gives a slope of 0.99, with an R^2 value of 0.99. The average absolute deviation of the comparison is 3.9 Wm^{-2}, with 62% of the estimated data falling within +/- 4 Wm^{-2} of the measurements. Thus it appears that this technique gives a reasonable estimation of the upwelling SW for Darwin.

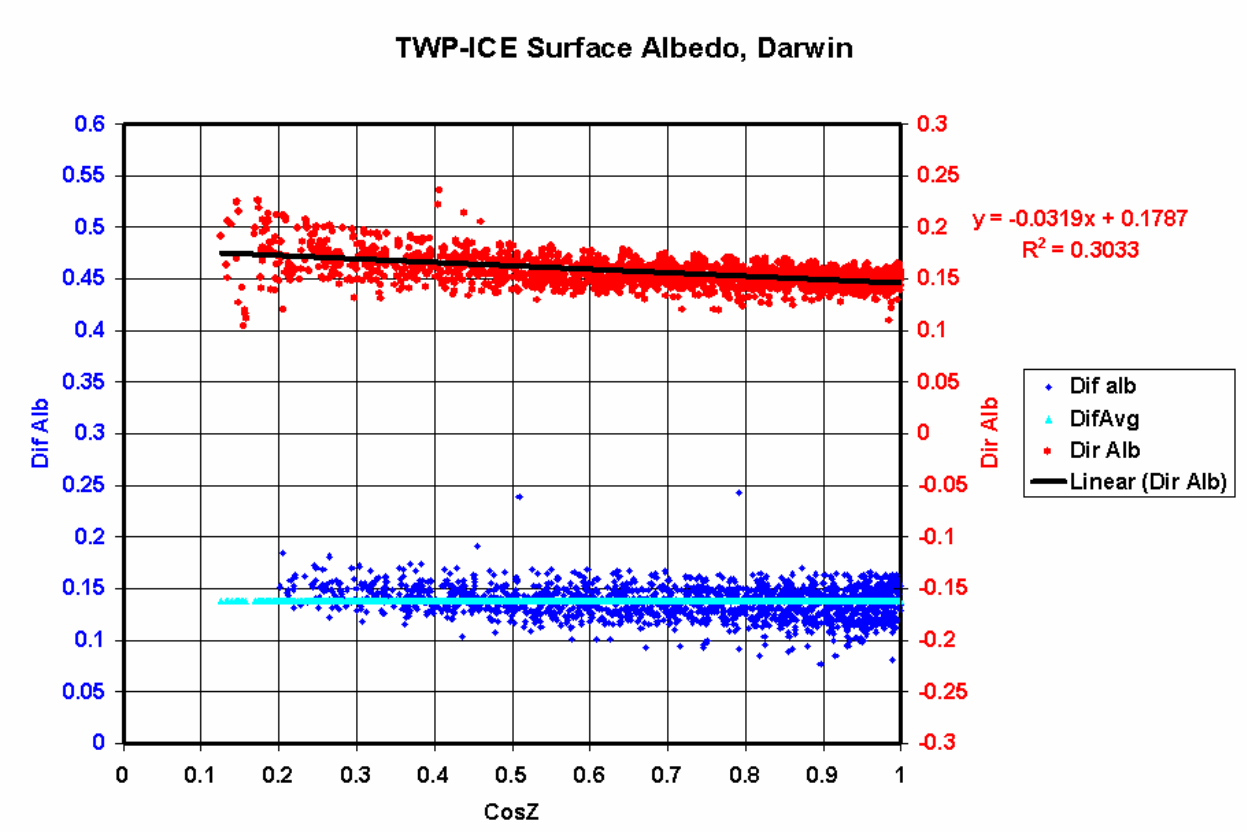

Figure 11: Measured SW surface albedo for Darwin site, separated by significant direct sun (red) and little direct sun (blue).

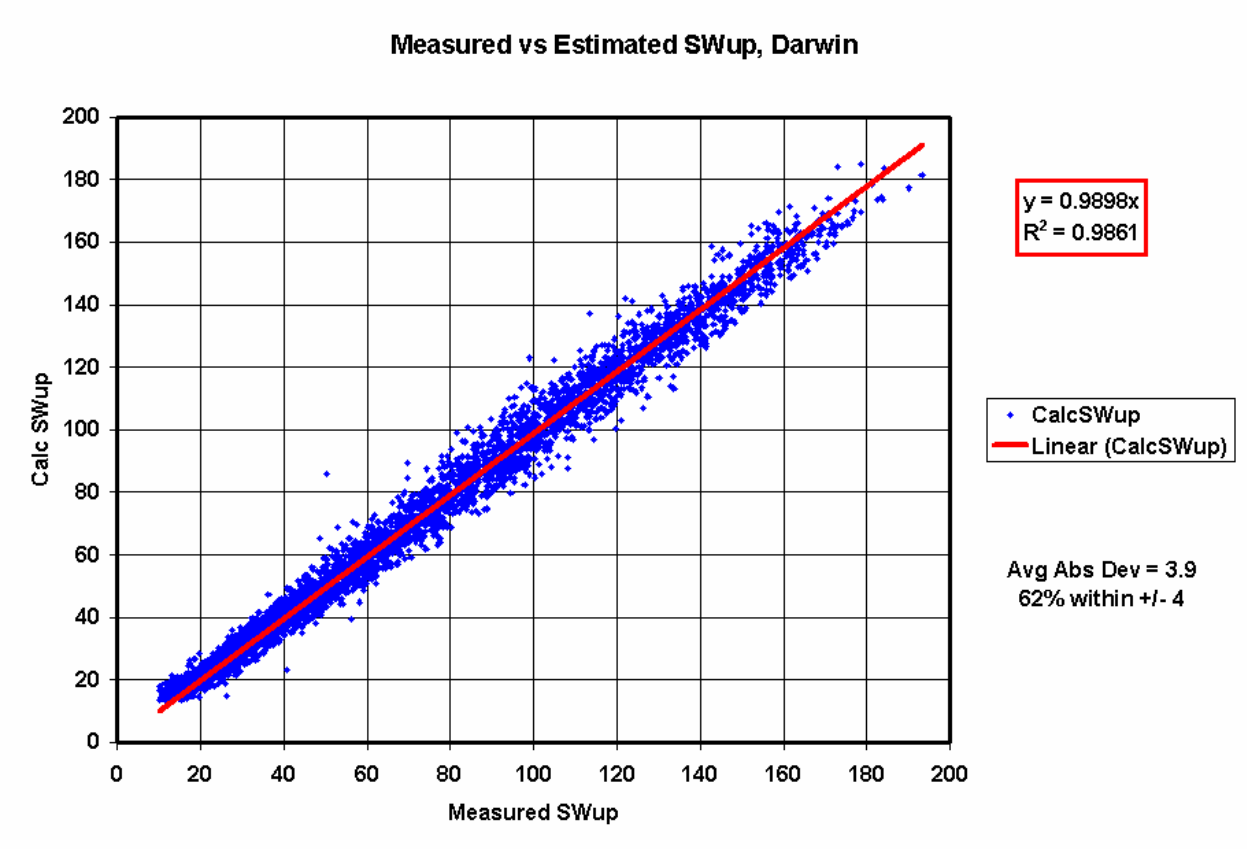

Figure 12: Comparison of estimated to measured upwelling SW for Darwin data.

Upwelling LW Relationship Determined Using Darwin Data

Estimation of the upwelling LW from the available downwelling radiation measurements is more complex than that for the upwelling SW. Where the relationship between SWdn and SWup is primarily radiative in nature, the LWup is a product of the total energy exchange at the surface. This energy exchange involves not only radiation, but also sensible and latent heat exchange as well. Additionally, especially for vegetated surfaces where the plants use some of the solar energy to produce sugars, the surface response to net SW (SWnet) is different than that to downwelling LW.

Typical dirt and vegetated land surfaces on average have a reasonably short response time to radiative changes, such that reasonably accurate clear-sky LWup estimations have been shown to be feasible (Long, 2005). [This is not the case for surfaces that are primarily water such as the Darwin Harbor and Fogg Dam sites, where thermal inertia and fluid effects significantly decrease the short-term correlation between changes in SWnet and LWdn to LWup variations.] Additionally, for the clear-sky case the variations in input radiative energies, as well as changes in latent and sensible heat partitioning, occur on relatively slower time scales than for the cloudy (especially partly cloudy for the radiative terms) sky case. For this reason estimation of the all-sky LWup shows greater uncertainty than that for the clear-sky LWup estimations shown in Long (2005).

As shown in Long (2005), the primary driver of the magnitude of the upwelling LW is the downwelling LW, primarily because absorptivity equals emmisivity for a given surface.

The next biggest term driving the variability of the upwelling LW amount is the net SW, followed by the latent and sensible heat terms. Thus as in Long (2005) fitting for the various terms used to estimate the LWup is done sequentially, i.e. the first fitting uses LWdn as the independent variable, then the residuals are fitted using the SWnet as the independent variable, etc. Where Long (2005) uses collocated measurements of relative humidity (RH) and wind speed as surrogates for information about the relative changes in radiative, latent, and sensible heat partitioning with respect to the upwelling LW, analysis of the Darwin wet season data show that the RH and wind speed terms add only some improvement to the estimation, with little gained by using both terms. The wind speed variable exhibits slightly greater correlation than the RH to the LWdn and SWnet estimated LWup residuals, and is used here as the third independent variable in the fitting.

On typical formula used for data quality assessment (Long and Dutton, 2002; Long and Shi, 2006) relates LWup to the ambient air temperature in the form

$$\sigma(T_a - C_1)^4 < LWup < \sigma(T_a + C_1)^4$$

Where σ is the Stephan-Boltzman constant, T_a is the ambient air temperature (in K), and C_1 is a constant. This formulation mimics the general "shape" of the typical LWup to T_a relationship boundaries. Adapting this formulation and fitting to the Darwin measured LWup data gives an offset constant of about 1.7 K. This fit line is shown in Figure 13 as the black dotted line. Obviously, this relationship is not alone sufficient for estimating the LWup measurements depicted as the blue diamonds. Subsequent sequential fitting as described previously yields the following formulas for estimating the LWup:

$$L1 = \sigma(Ta + 1.7017)^4 \quad (3)$$
$$L2 = L1 + 0.0493*SWdn - 2.6 \quad (4)$$
$$LWup = L2 - 0.8747* Wspd + 2.0 \quad (5)$$

Where L1 is the result using Ta alone, L2 is the result after including the SWnet term, and LWup is the final estimated LWup. Figure 14 shows a comparison, similar to Figure 12, but for measured and estimated upwelling LW. An RMS fitted line through the comparison forced through zero gives a slope of 0.999, with an R^2 value of 0.906. While Figure 14 shows what appears to be a larger scatter than that in Figure 12, it should be noted that 82% of the more than 11,200 data points in the plot fall below the 500 Wm^{-2} range which exhibits less scatter than the data in the range above 500 Wm^{-2}. Thus the average absolute deviation of the comparison is still only 5.3 Wm^{-2}, with 70% of the estimated data falling within +/- 6 Wm^{-2} of the measurements. This again seems a reasonable agreement given the complexity of the surface energy exchange of which the LWup is only one term.

Comparison of Radiative Energy Budget Results

Applying Equations 1 through 5 to the Cape Don and Garden Point data as appropriate allows a comparison of the surface radiative energy budget terms to the Darwin measurements. Figure 15 shows the daily average downwelling and upwelling SW for

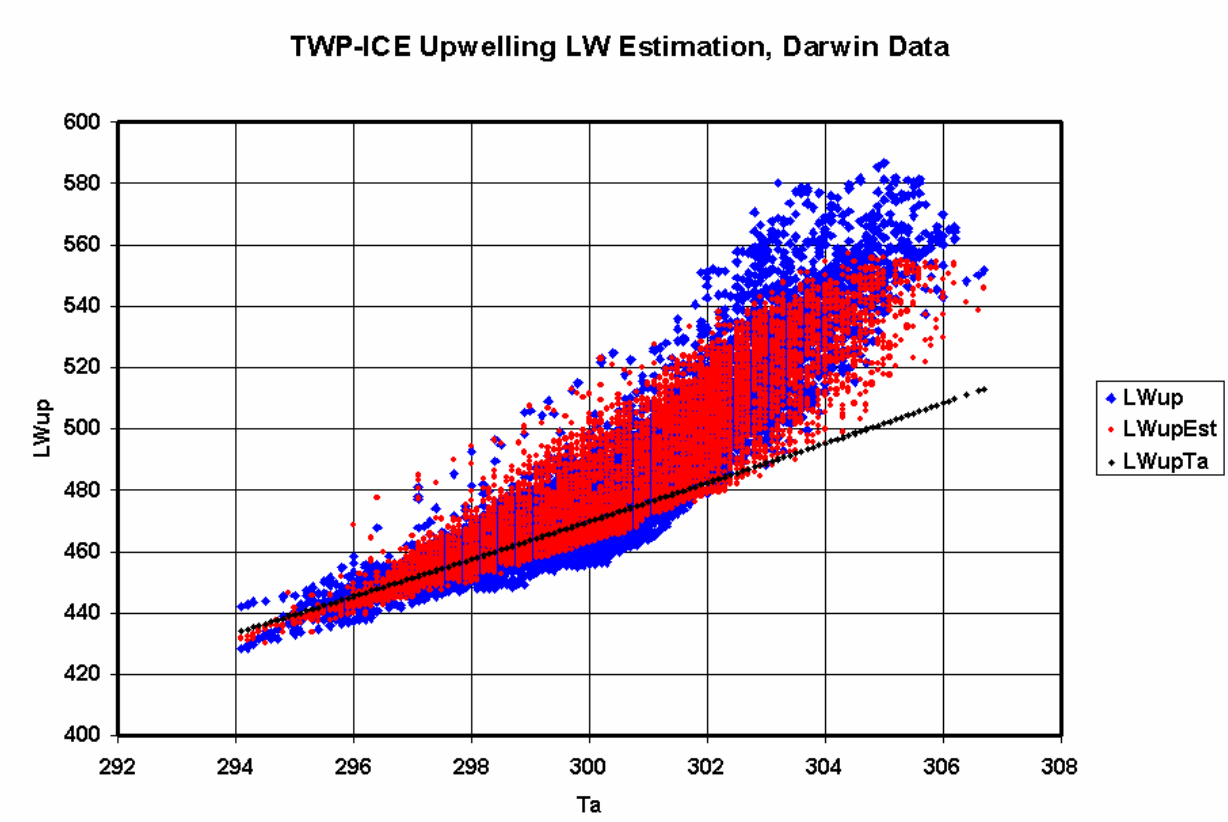

Figure 13: Measured and estimated LWup versus air temperature for Darwin data.

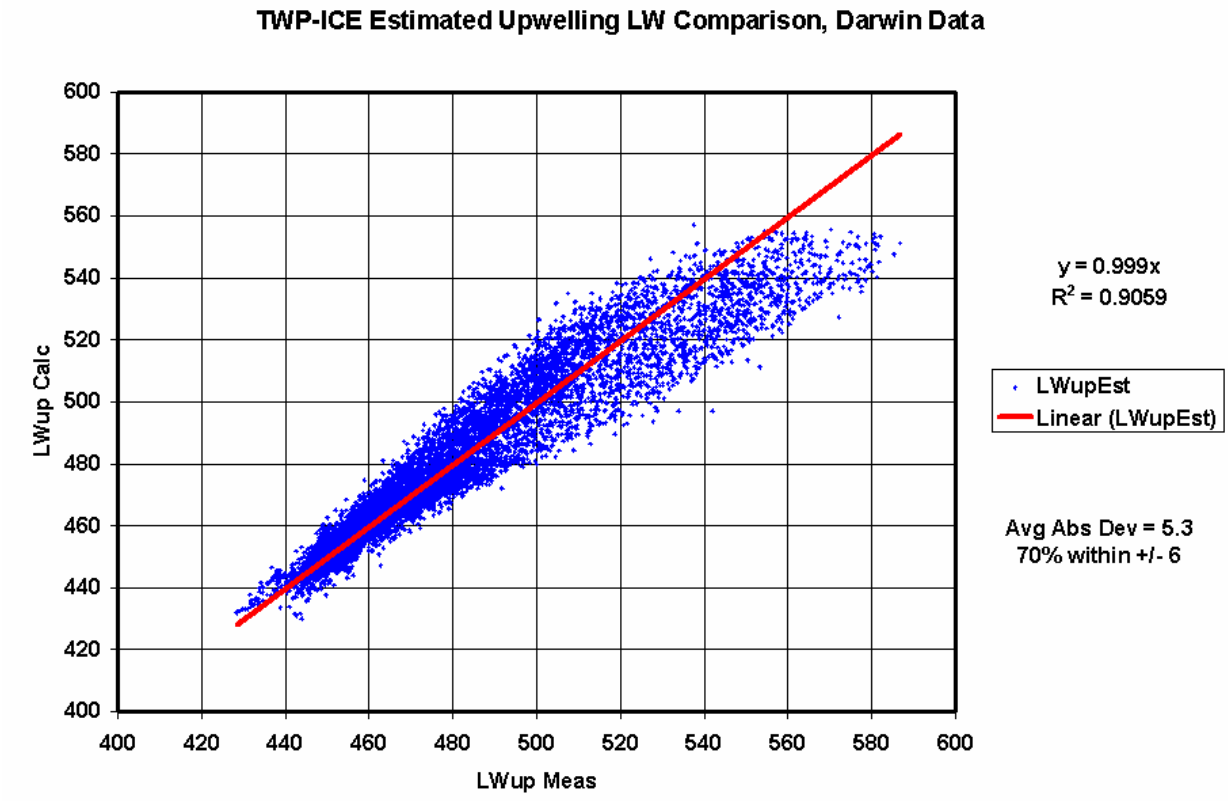

Figure 14: Comparison of estimated to measured upwelling LW for Darwin data.

the three sites. Overall, this plot shows the effect of cloudiness changes during TWP-ICE where the overall meteorological conditions evolved from active monsoon conditions through a regime dominated by a persistent and intense low pressure system to the south of Darwin, to a regime with dry atmosphere above the boundary layer suppressing cloud formation, and then monsoon break conditions. As a result of this evolution of sky conditions, in general the three sites experienced a greater effect of clouds on the surface radiative energy budget in the first half of TWP-ICE than in the second half. Within this overall evolution for the TWP-ICE domain, there are site-to-site variations. For example for January 18 - 20 both Cape Don and Garden Point show greater daily downwelling SW amounts than Darwin, indicating less cloudiness for these more northern sites. The opposite occurs for the days from February 2 - 5, with Darwin downwelling SW amounts being greater. The upwelling SW being driven by the SWdn amounts, this same relative pattern exists for the SWup as well.

As noted by Ohmura (2001), typically 60-70% of the surface clear-sky downwelling LW is produced within the lowest 100 meters of the atmosphere above the detector, with 90% being produced in the lowest kilometer. Due to the large column water vapor amounts and warm atmospheric temperatures of the tropics the downwelling clear-sky LW typically averages around 400 Wm^{-2} or more for the ARM equatorial sites, and the Darwin wet season as well. In this atmospherically "soupy" regime, clouds exhibit far less influence on the downwelling LW than for the SWdn. Thus, the variability in LWdn is comparatively small, as shown in Figure 16 where despite the Y axis scale being half that of Figure 15, the variability is still visually far less than for the SWdn. Figure 16 also shows the influence of the SWnet on the upwelling LW, where as the daily average SWdn increases (Fig. 15) toward the end of the TWP-ICE period, there is a corresponding increase in the upwelling LW even though there is a decrease in the LWdn.

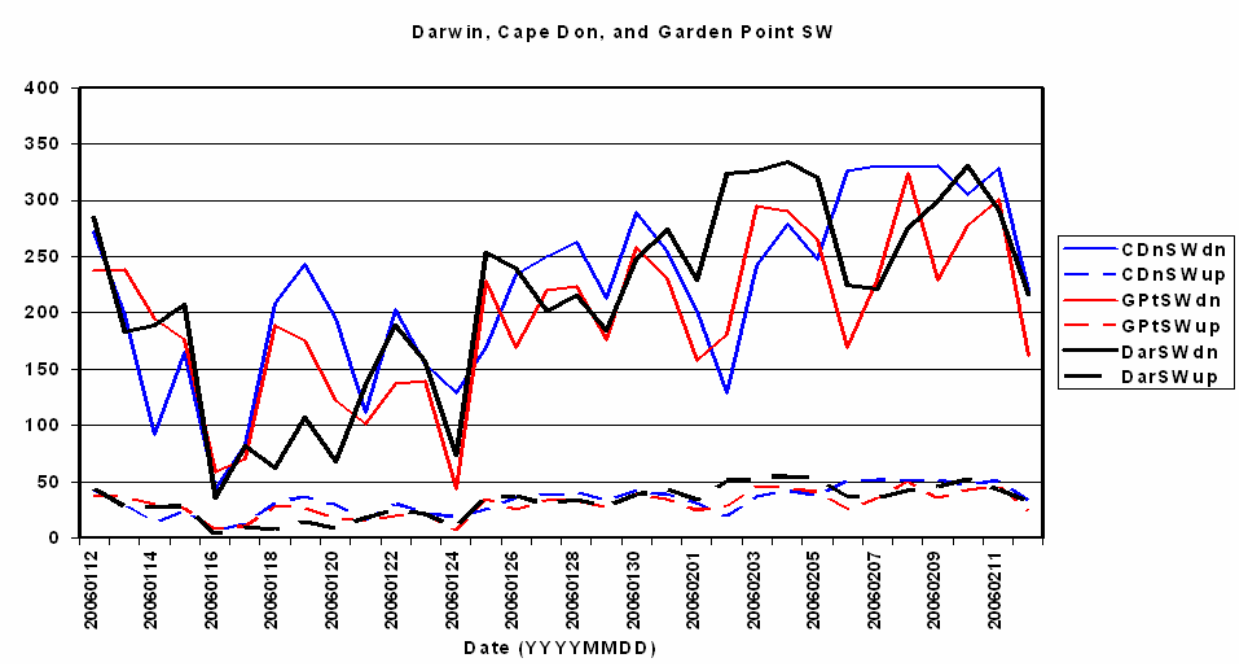

Figure 15: Daily average SWdn and SWup for the three study sites during TWP-ICE.

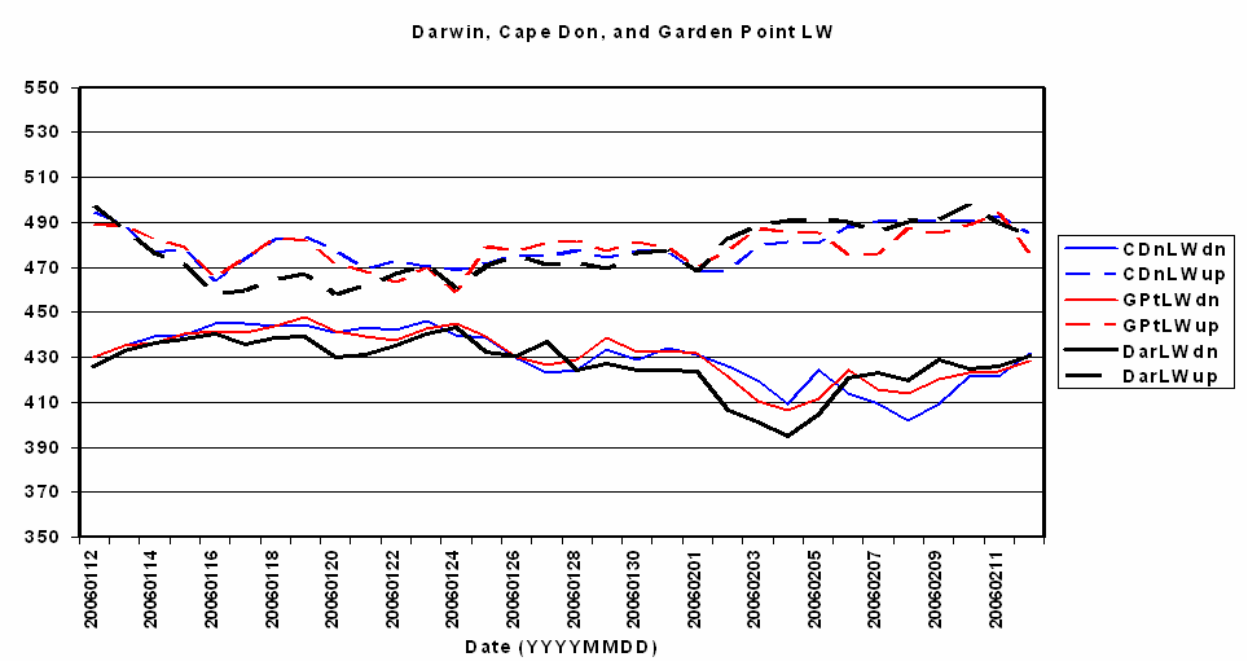

Figure 16: Daily average LWdn and LWup for the three study sites during TWP-ICE.

Calculating the net irradiance as the downwelling minus the upwelling for the SW and LW components shown in Figures 15 and 16 gives the component net values shown in Figure 17. Since the LWup is greater in magnitude than the LWdn, the net LW effect is a loss of energy at the surface. The opposite is true for the net SW, though the net SW gain is greater than the net LW loss, so that in the aggregate the surface experiences a net gain in energy. The net LW loss is negatively correlated with the net SW gain over the TWP-ICE period. As discussed previously there are differences between the three sites on a daily basis, but similar overall changes over the TWP-ICE period. In the aggregate the three sites exhibit very similar net LW, with the overall net LW averages being -49 Wm^{-2}, -48 Wm^{-2}, and -50 Wm^{-2} for Cape Don, Garden Point, and Darwin, respectively. There are greater differences for the net SW, with the overall averages being 186 Wm^{-2}, 166 Wm^{-2}, and 180 Wm^{-2} for Cape Don, Garden Point, and Darwin, respectively. The greater net SW for Cape Don is produced by the less cloudy skies that occurred there toward the end of TWP-ICE, where at the same time the occurrence of the Hector convective phenomenon comparatively decreased the net SW at Garden Point. The total net surface radiative energy budget is calculated as the sum of the net SW and LW terms, and is shown in Figure 18. Because the net SW and net LW are anti-correlated, the total net radiative change is somewhat smaller than that for the net SW across the TWP-ICE period, yet is dominated by the net SW term. The overall averages for the surface radiative energy budget are 137 Wm^{-2}, 118 Wm^{-2}, and 130 Wm^{-2} for Cape Don, Garden Point, and Darwin, respectively.

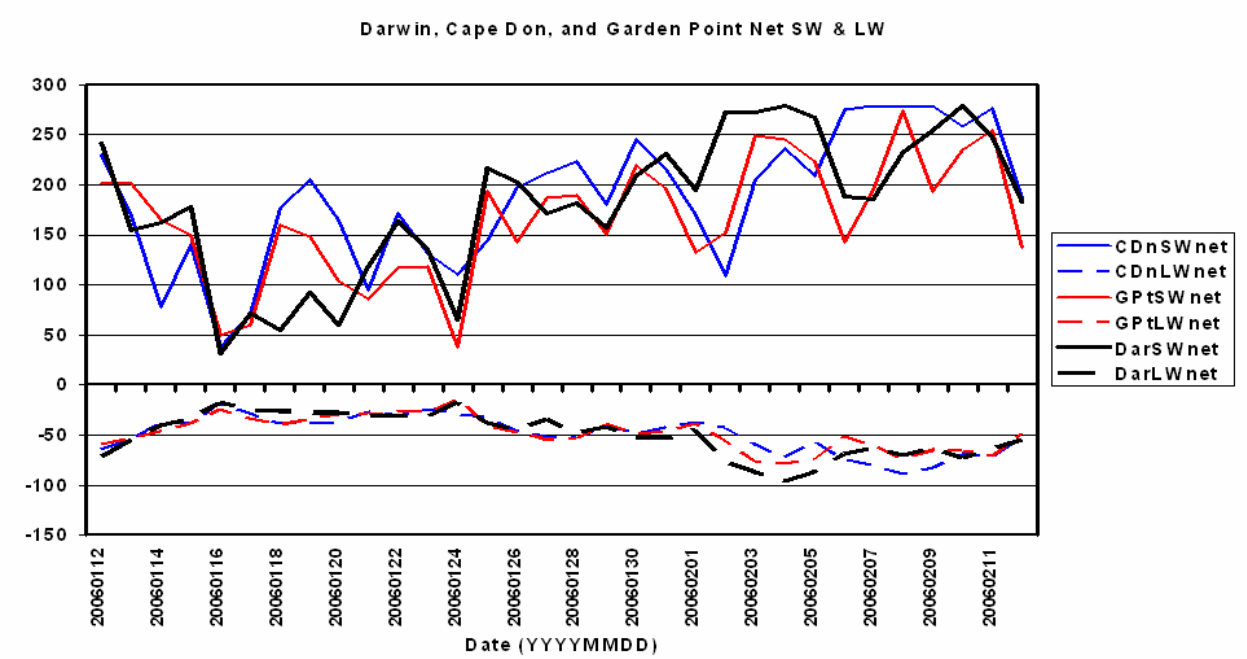

Figure 17: Daily average net SW and LW for the three study sites during TWP-ICE.

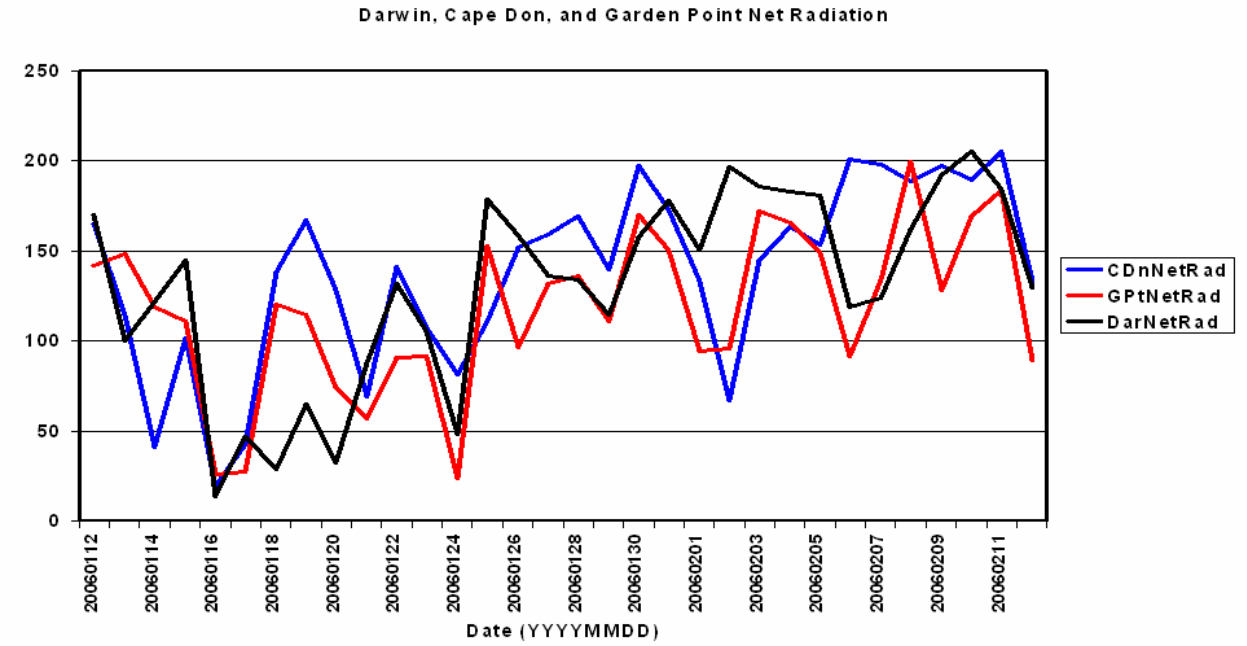

Figure 18: Daily average total net surface radiative energy budget for the three study sites during TWP-ICE.

Summary

Relationships with various Darwin data have been calculated with the aim of estimating the upwelling SW and LW components for the Cape Don and Garden Point sites for the TWP-ICE period. The relationships are shown to be able to estimate the upwelling Darwin data wherein 62% of the estimated data fall within +/- 4 Wm^{-2} of the

measurements for the upwelling SW, and with 70% of the estimated data falling within +/- 6 Wm^{-2} of the measurements for the upwelling LW. Photographic evidence shows that the surface in the field-of-view of the downward facing radiometers at Darwin is similar to that in the immediate area surrounding the radiometers at Cape Don and Garden Point. However, this same photographic evidence also shows that for all three sites the question of how representative the upwelling measurements or estimates are of the larger area is problematic, as is always the case for upwelling measurements.

Analysis using the derived relationships to estimate the Cape Don and Garden Point upwelling SW and LW show reasonable comparison to the Darwin data for the TWP-ICE period. Thus, while no estimation of the additional uncertainty associated with surface property differences is possible due to lack of comparative measurements, the upwelling estimates do seem to reside “in the ballpark” and are offered as such.

References

Long, C. N. and E. G. Dutton, (2002): BSRN Global Network recommended QC tests, V2.0, BSRN Technical Report, available via (http://ezksun3.ethz.ch/bsrn/admin/dokus/qualitycheck.pdf)

Long, C. N., (2005): On the Estimation of Clear-Sky Upwelling SW and LW, 15th ARM Science Team Meeting Proceedings, Daytona Beach, Florida, March 14-18, 2005.

Long, C. N. and Y. Shi, (2006): The QCRad Value Added Product: Surface Radiation Measurement Quality Control Testing, Including Climatologically Configurable Limits, Atmospheric Radiation Measurement Program Technical Report, ARM TR-074, 69 pp., Available via http://www.arm.gov/publications/techreports.stm.

Ohmura, A. (2001): Physical basis for the temperature/melt-index method, JAM, 40 ; pp 753-761.